

 $k_{\perp}^{-8/3}$ **Spectrum in Kinetic Alfvén Wave Turbulence: Implications for the Solar Wind**Vincent David^{1,2} and Sébastien Galtier^{1,2,3} ¹ Laboratoire de Physique des Plasmas, École polytechnique, F-91128 Palaiseau Cedex, France; sebastien.galtier@u-psud.fr² Univ. Paris-Sud, Observatoire de Paris, Univ. Paris-Saclay, CNRS, Sorbonne Univ., France³ Institut universitaire de France, France

Received 2019 June 3; revised 2019 July 1; accepted 2019 July 8; published 2019 July 19

Abstract

The nature of solar wind turbulence at large scale is rather well understood in the theoretical framework of magnetohydrodynamics. The situation is quite different at subproton scales where the magnetic energy spectrum measured by different spacecraft does not fit with the classical turbulence predictions: a power-law index close to $-8/3$ is generally reported, which is far from the predictions of strong and wave turbulence, $-7/3$ and $-5/2$, respectively. This discrepancy is considered as a major problem for solar wind turbulence. Here, we show with a nonlinear diffusion model of weak kinetic Alfvén wave turbulence where the cascade is driven by local triadic interactions that a magnetic spectrum with a power-law index of $-8/3$ can emerge. This scaling corresponds to a self-similar solution of the second kind with a front propagation following the law $k_f \sim (t_* - t)^{-3/4}$, with $t < t_*$. This solution appears when we relax the implicit assumption of stationarity generally made in turbulence. The agreement between the theory and observations can be interpreted as an evidence of the nonstationarity of solar wind turbulence at subproton scales.

Key words: plasmas – solar wind – turbulence – waves

1. Introduction

The solar wind is a collisionless plasma characterized by fluctuations of its primary fields over a huge range of frequencies. One of the most spectacular properties reported from in situ measurements is a spectrum of magnetic fluctuations from frequencies $f \sim 10^{-6}$ Hz to ~ 100 Hz (Kiyani et al. 2015) with a spectral break around $f_b \sim 1$ Hz (Behannon 1978; Denskat et al. 1983; Leamon et al. 1998; Bourouaine et al. 2012; Chen et al. 2014). This break separates the magnetohydrodynamic (MHD) scales ($f < f_b$) from the subproton scales ($f > f_b$) where ions and electrons are decoupled, and where signatures of kinetic Alfvén waves (KAWs) can be found (see, e.g., Sahraoui et al. 2010; Salem et al. 2012; Chen et al. 2013). Note that signatures of other types of waves are also found (see, e.g., Narita et al. 2011; Roberts & Li 2015). Despite several years of studies, the nature of solar wind turbulence at subproton scales remains under debate (in this Letter we restrict our attention to scales greater than the electron gyroscale). A reason is that the magnetic energy spectrum reported is generally close to $f^{-8/3}$ (Alexandrova et al. 2012; Podesta 2013; Sahraoui et al. 2013), which is far from the classical predictions of strong and (weak) wave turbulence (Biskamp et al. 1996; Galtier & Bhattacharjee 2003; Galtier 2006a, 2006b; Schekochihin et al. 2009; Voitenko & de Keyser 2011; Galtier & Meyrand 2015; Cerri et al. 2016; Passot et al. 2018) for which the power-law indices are $-7/3$ and $-5/2$, respectively.

A debate is also developed around the mechanisms of energy dissipation. Although it seems necessary to heat the interplanetary collisionless plasma to explain its nonadiabatic cooling (Richardson et al. 1995), the precise mechanism that involves kinetic effects is still not totally understood. For example, we do not know if some dissipation occurs in the inertial range where a spectrum close to $f^{-8/3}$ is found. A possibility is that the latter power law is a spectrum predicted by a classical turbulence theory modified by some kinetic dissipation (see, e.g., Passot & Sulem 2015). Note that several

studies have been devoted to the question of solar wind heating and the evaluation of the energy cascade rate at MHD scales, which can be seen as a proxy for measuring the heating rate (see, e.g., Sorriso-Valvo et al. 2007; Vasquez et al. 2007; MacBride et al. 2008; Osman et al. 2011; Banerjee et al. 2016; Hadid et al. 2017).

The Letter is organized as follows. In Section 2 we introduce a model of KAW turbulence, first derived by Passot & Sulem (2019), and its phenomenology. In Section 3 we present its nonstationary solution, which is a self-similar solution of the second kind. The numerical validation of our theory is given in Section 4. A discussion is given in Section 5 about the applications to solar wind turbulence at subproton scales. A conclusion is finally proposed in the last section.

2. Model of KAW Turbulence

Nonlinear diffusion models are often used in the analysis of both strong (Leith 1967; Connaughton & Nazarenko 2004; Matthaeus et al. 2009; Thalabard et al. 2015) and weak wave turbulence (Zakharov & Pushkarev 1999; Boffetta et al. 2009; Galtier et al. 2019). These are mostly built by using phenomenological arguments, but a rigorous treatment is sometimes possible in the regime of wave turbulence. The known examples are nonlinear optics (Dyachenko et al. 1992) and MHD (Galtier & Buchlin 2010). In this case, the nonlinear diffusion equations are derived by taking the strongly local interaction limit of the kinetic equations; the latter equations themselves being derived in a systematical way. Recently, such a model has been proposed by Passot & Sulem (2019) for KAW turbulence (a model also valid for oblique whistler waves as explained in Galtier & Meyrand 2015) neglecting the coupling to other types of waves. The derivation can be qualified as semianalytical because the problem is fundamentally anisotropic and in the final step of the derivation the authors neglected the cascade along the uniform magnetic field to find an expression for the nonlinear diffusion equation. However, the parallel cascade is expected to be relatively weak

and its absence cannot be seen as a drawback of the model. Then, KAW turbulence is simulated numerically in the presence of magnetic helicity in order to study the regime of imbalanced weak turbulence (Passot & Sulem 2019). This type of model gives in general good quantitative information about the primary system because local interactions are in general the main driver of the turbulence cascade.

Here, we shall use the diffusion equation proposed by Passot & Sulem (2019) for weak KAW turbulence in the absence of magnetic helicity. To be self-consistent (and for pedagogical reasons) a new derivation is proposed by using only phenomenological arguments. This method has the advantage of explaining in a simple way the main physical ingredients required to derive a nonlinear diffusion model for KAW turbulence.

Since the leading nonlinear interaction of KAW is a three-wave interaction (Galtier & Meyrand 2015; Passot & Sulem 2019), the model is a second-order diffusion equation of the type

$$\frac{\partial E(k_{\perp})}{\partial t} = \frac{\partial}{\partial k_{\perp}} \left[D_{k_{\perp}} E(k_{\perp}) \frac{\partial(E(k_{\perp})/k_{\perp})}{\partial k_{\perp}} \right], \quad (1)$$

where $E(k_{\perp})$ is a one-dimensional magnetic energy spectrum, k_{\perp} the perpendicular wavenumber, and $D_{k_{\perp}}$ a diffusion coefficient that eventually depends on the wavenumber k_{\perp} . This equation is constructed in such a way that it preserves the nonlinearity degree with respect to the spectrum (quadratic in our case) and its cascade and thermodynamic solutions. We neglect the cascade along the strong uniform magnetic field \mathbf{B}_0 which defines the parallel direction, hence the presence of only the perpendicular (to \mathbf{B}_0) wavenumber k_{\perp} . A dimensional analysis of expression (1) gives

$$\frac{E(k_{\perp})}{\tau} \sim \frac{D_{k_{\perp}} E^2(k_{\perp})}{k_{\perp}^3}, \quad (2)$$

where τ is the cascade time of weak wave turbulence; thus,

$$D_{k_{\perp}} \sim \frac{k_{\perp}^3}{\tau E(k_{\perp})} \sim \frac{k_{\perp}^3}{(\tau_{\text{KAW}}/\epsilon^2) E(k_{\perp})}. \quad (3)$$

The KAW time is given by the relation

$$\tau_{\text{KAW}} \sim \frac{1}{\omega} \sim \frac{1}{k_{\parallel} k_{\perp}} \sim \frac{1}{k_{\perp}}, \quad (4)$$

where $\epsilon \sim \tau_{\text{KAW}}/\tau_{\text{NL}} \ll 1$ is a small parameter and the nonlinear time $\tau_{\text{NL}} \sim 1/(k_{\perp}^2 \sqrt{k_{\perp} E(k_{\perp})})$. We obtain

$$D_{k_{\perp}} \sim k_{\perp}^7, \quad (5)$$

which leads to the following second-order diffusion equation for KAW turbulence (Passot & Sulem 2019):

$$\frac{\partial E(k_{\perp})}{\partial t} = C \frac{\partial}{\partial k_{\perp}} \left[k_{\perp}^7 E(k_{\perp}) \frac{\partial(E(k_{\perp})/k_{\perp})}{\partial k_{\perp}} \right], \quad (6)$$

where C is a positive constant.

The constant flux solutions can now be found. We define the energy flux $\Phi_E(k_{\perp})$ as follows:

$$\frac{\partial E(k_{\perp})}{\partial t} = - \frac{\partial \Phi_E(k_{\perp})}{\partial k_{\perp}} \quad (7)$$

and introduce the magnetic energy spectrum $E(k_{\perp}) = A k_{\perp}^x$ into Equation (6) with A , a positive constant. We find

$$\Phi_E(k_{\perp}) = A^2 C (1-x) k_{\perp}^{5+2x}. \quad (8)$$

The constant flux solutions are $x = 1$, which corresponds to the thermodynamic solution (zero flux), and $x = -5/2$ called the Kolmogorov–Zakharov solution (Nazarenko 2011). In this case we also find $\Phi_E(k_{\perp}) \equiv \Phi_0 = (7/2) A^2 C$, which is positive and thus corresponds to a direct cascade. Therefore, we recover the well-known solutions of the problem (Galtier & Bhattacharjee 2003; Galtier & Meyrand 2015; Passot & Sulem 2019).

3. Nonstationary Regime

Time-dependent solutions of the KAW turbulence Equation (6) will be studied further analytically and numerically. We will demonstrate the existence of a nontrivial solution (sometimes called anomalous scaling) in the sense that it cannot be derived with the usual turbulence phenomenology or theory. This property is related to the finite capacity of the system, which is linked to the convergence of the integral

$$\int_{k_i}^{+\infty} E(k_{\perp}) dk_{\perp}, \quad (9)$$

where k_i is the scale of magnetic energy injection. This property is satisfied when $x < -1$, a situation found in KAW turbulence.

The nonstationary spectrum can be modeled as a self-similar solution of the second kind (see, e.g., Falkovich & Shafarenko 1991; Thalabard et al. 2015), taking the form

$$E(k_{\perp}) = \frac{1}{\tau^a} E_0 \left(\frac{k_{\perp}}{\tau^b} \right), \quad (10)$$

where $\tau = t_* - t$, and t_* is a finite time at which the magnetic energy spectrum reached the largest available wavenumber. By introducing the above expression into (6) we find the condition

$$a = 4b + 1. \quad (11)$$

A second condition can be found by assuming that $E_0(\xi) \sim \xi^m$ far behind the front. Then, the stationarity condition gives the following relation:

$$a + mb = 0. \quad (12)$$

Finally, the combination of both relations gives

$$m = -\frac{a}{b} = -4 - \frac{1}{b}. \quad (13)$$

The latter expression means that we have a direct relation between the power-law index m of the spectrum and the law of the front propagation that follows $k_f \sim \tau^b$. For example, if we assume that the stationary solution—the Kolmogorov–Zakharov spectrum—is established immediately during the front propagation, then $m = -5/2$ and $b = -2/3$ (and $a = -5/3$). In this case, the prediction for the front propagation is

$$k_f \sim (t_* - t)^{-2/3}. \quad (14)$$

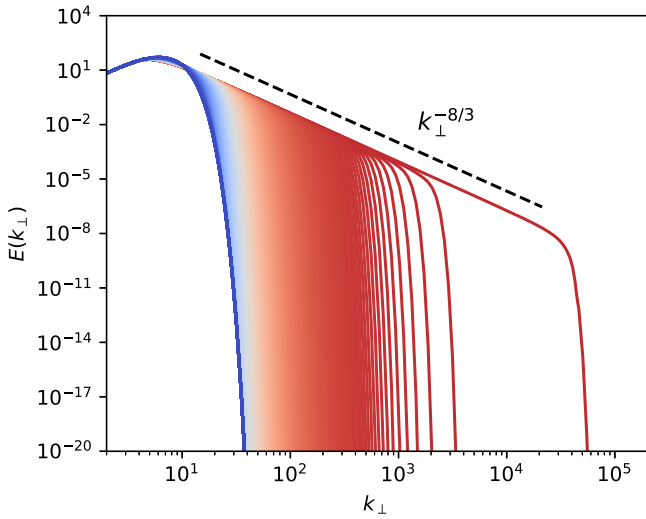


Figure 1. Time evolution (every $1000dt$) of the magnetic energy spectrum $E(k_{\perp})$ from $t = 0$ (blue) to t_* (dark red). A $k_{\perp}^{-8/3}$ spectrum emerges over three decades.

4. Numerical Simulation

We now study numerically the time evolution of the magnetic energy spectrum described by the KAW turbulence Equation (6) with $C = 1$. A linear hyperviscous term of the form $-\eta k_{\perp}^6 E(k_{\perp})$ is added to Equation (6) in order to introduce a sink at small scale to avoid the development of numerical instabilities at the final time of the simulation ($t > t_*$) when the stationary state establishes; we take $\eta = 10^{-16}$. A logarithmic subdivision of the k_{\perp} -axis is used with $k_{\perp i} = 2^{i/8}$ and i an integer varying between 0 and 160. Note that this resolution is far too large to model the subproton scales where electron inertia is neglected. This choice is, however, necessary to reach a clear conclusion about the values of the power-law indices (see below). The Crank–Nicholson and Adams–Bashforth numerical schemes are implemented for the nonlinear and dissipative terms, respectively. The initial condition ($t = 0$) corresponds to a spectrum localized at large scale with $E(k_{\perp}) \sim k_{\perp}^3 \exp(-(k_{\perp}/k_0)^2)$ and $k_0 = 5$. No forcing is added at $t > 0$. The time step is $dt = 2 \times 10^{-13}$.

In Figure 1 we show the time evolution of the magnetic energy spectrum from $t = 0$ to t_* . During this nonstationary phase a clear power-law spectrum in $k_{\perp}^{-8/3}$ is formed behind the front. To check if this spectrum corresponds to the self-similar solution of the second kind introduced above we show in Figure 2 the front propagation $k_f(t)$. This front is defined by taking $E(k_{\perp}) = 10^{-15}$ from Figure 1: we then follow the point of intersection between this threshold and the spectral tail. From Figure 2 we can define the singular time t_* at which the front, in principle, can reach $k_{\perp} = +\infty$. Note that a similar situation where the small scales are reached in a finite time is also observed, e.g., in Alfvén wave turbulence (Galtier et al. 2000). The value $t_* = 6.7537 \times 10^{-7}$ is chosen. In Figure 2 (inset) we show k_f as a function of $t_* - t$: a clear power law is observed over three decades with a power-law index of -0.750 . The negative value illustrates the explosive character of the direct cascade of magnetic energy in KAW turbulence. The different values measured are fully compatible with

$$a = -2, \quad b = -3/4 \quad \text{and} \quad m = -8/3, \quad (15)$$

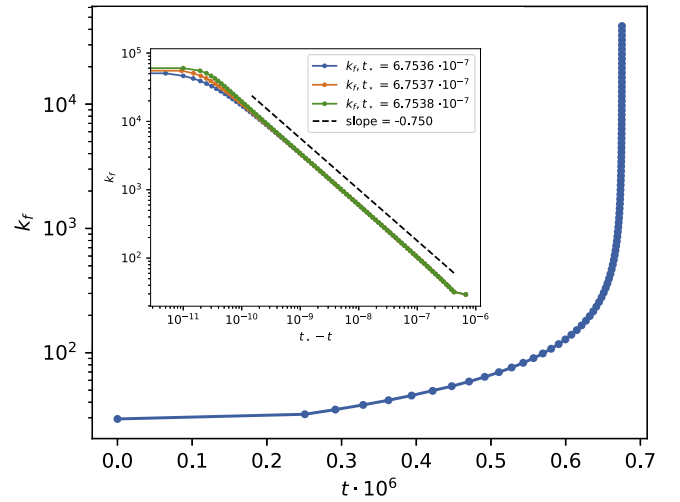


Figure 2. Temporal evolution of the spectral front k_f for $t \leq t_*$ in linear-logarithmic coordinates (blue). A sharp increase of k_f is observed from which we can define precisely the singular time $t_* = 6.7537 \times 10^{-7}$. Inset: the temporal evolution of k_f as a function of $t_* - t$ (orange) in double logarithmic coordinates. The black dashed line corresponds to $(t_* - t)^{-0.750}$. For comparison two other values of t_* are taken (green and blue).

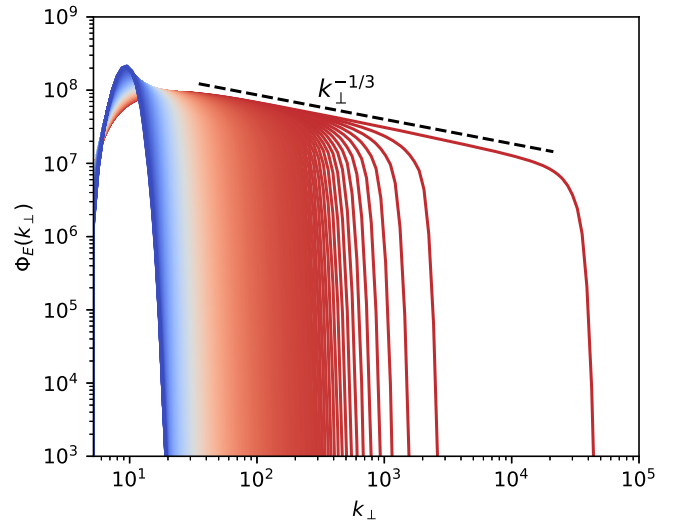


Figure 3. Temporal evolution of the energy flux $\Phi_E(k_{\perp})$ in double logarithmic coordinates for the same times as in Figure 1 (same conventions). The flux follows a power law $\sim k_{\perp}^{-1/3}$.

which therefore demonstrates the self-similar nature of the nonstationary solution.

As displayed in Figure 3, the nonstationary phase is characterized by a nonconstant energy flux $\Phi_E(k_{\perp})$ (computed from the nonlinear terms): we start with a flux localized at small wavenumbers that then develops toward smaller scales without reaching a plateau. The solution does not correspond to the constant flux solution derived analytically, but it is fully compatible with the power-law solution $\sim k_{\perp}^{-1/3}$ when we take $x = -8/3$ in Equation (8).

Finally, in Figure 4 we show the temporal evolution for $t > t_*$ of the energy spectrum and energy flux (inset), respectively. The classical (stationary) wave turbulence predictions are finally obtained with an energy spectrum in $k_{\perp}^{-5/2}$ and a constant positive energy flux, as expected for a direct cascade. This behavior is specific to a viscous simulation

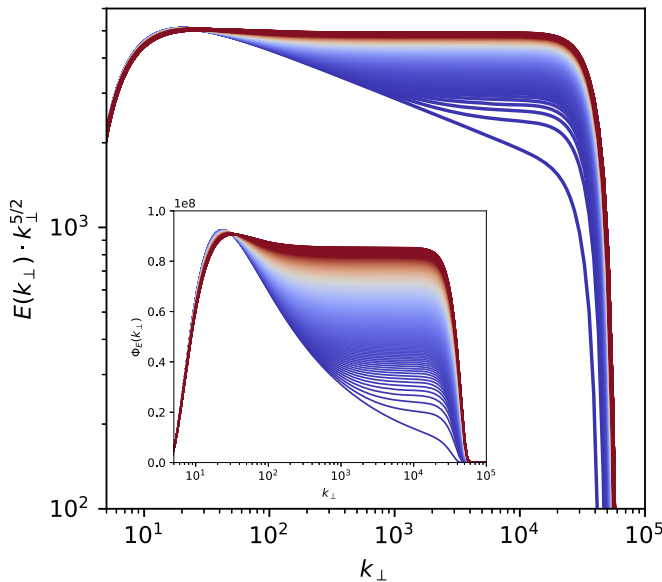


Figure 4. Temporal evolution (every $1000dt$) for $t > t_*$ of the energy spectrum compensated by $k_{\perp}^{5/2}$ (in double logarithmic coordinates). Inset: temporal evolution of the energy flux $\Phi_E(k_{\perp})$ for the same times (in linear-logarithmic coordinates).

made in a finite box where the cascade cannot continue to smaller scales: the energy accumulates at small scale until the viscous term (proportional to the energy spectrum) becomes nonnegligible and balances the energy flux coming from large scale. This process affects the entire inertial range with a modification of the power-law index. The final phase of the simulation (not shown) corresponds to a self-similar decay of the energy spectrum with the same power-law index ($-5/2$).

5. Solar Wind Turbulence at Subproton Scales

Solar wind turbulence at subproton scales (for frequencies $f > 1$ Hz) is characterized by a magnetic energy spectrum with a power-law index close to $-8/3$ (Alexandrova et al. 2012; Podesta 2013; Sahraoui et al. 2013). This scaling law does not correspond to the classical prediction of strong turbulence ($-7/3$) or weak wave turbulence ($-5/2$), which are obtained phenomenologically or analytically, respectively, with different types of model equations, and with different types of waves, in the presence of anisotropy or not. After several years of investigations, the possibility of having a power-law index close to the data seemed to be impossible with the classical turbulence theory (see, however, Boldyrev & Perez 2012; Meyrand & Galtier 2013). For this reason, this problem is one of the most important in space plasma physics. A natural conclusion is that the observed power laws are the result of a nontrivial turbulent dynamics that we still do not understand or a physics involving ingredients other than turbulence.

In this Letter, we have shown with a nonlinear diffusion model of weak KAW turbulence, which retains only local interactions (Passot & Sulem 2019), that by relaxing the implicit assumption of stationarity generally made in turbulence to obtain predictions, a new solution—a self-similar solution of the second kind—is possible for KAW turbulence. It is characterized by a magnetic energy spectrum in $k_{\perp}^{-8/3}$ that coincides with in situ observations. In this nonstationary phase the viscous dissipation is negligible. While the absence of viscous dissipation should be considered as the right way to

tackle the problem of solar wind turbulence at subproton scales, since the solar wind is a collisionless plasma and thus cannot behave like a viscous fluid, we must nevertheless clarify the meaning and the consequences of such assumption. The first clear idea is that there is no reason to believe that dissipation at kinetic scales should behave like that found in hydrodynamics; Landau damping is a good example. According to our interpretation the results obtained here are in favor of a kinetic dissipation that does not produce a feedback on the inertial range of KAW turbulence. This property is at odds with fluid turbulence. We might also conclude that the kinetic dissipation is simply negligible; however, the presence of kinetic dissipation as a source of plasma heating seems to be necessary to explain the slow (ion) temperature variation with the heliocentric distance (Richardson et al. 1995). According to our study, we can also think that the observation of a spectral index close to $-8/3$ in the solar wind is a consequence of the existence of a cascade at electron scale since in this case the accumulation of magnetic energy found in our simulation is not favored. The physics at electron scales is, however, quite different: for example the magnetic energy is not an invariant anymore (see, e.g., Meyrand & Galtier 2010). Then, the feedback of these scales on the ion scales studied in this paper is nontrivial. Note, finally, that the weak turbulence regime studied in this Letter also provides a natural explanation to the enigmatic non-Gaussian monoscaling observed at subproton scales (Kiyani et al. 2009).

6. Conclusion

Our study reveals that the classical hypothesis of stationarity to obtain any turbulence predictions may not be the best way to understand solar wind turbulence at subproton scales. Instead, the relaxation of this assumption opens a new type of solution that is understood as a self-similar solution of the second kind. On the basis of numerical simulations of a nonlinear diffusion model of weak KAW turbulence we show that the main scaling behavior observed with spacecraft—a power-law index close to $-8/3$ for the magnetic energy spectrum—which has so far resisted classical theoretical modeling, can be reproduced with a fairly high accuracy. The nonstationary nature of solar wind turbulence at subproton scales can be explained by an imbalance between nonlinearities and kinetic dissipation, and by the existence of a cascade at electron scales. The nature of the kinetic dissipation in a collisionless plasma remains to be explained in detail to fit these constraints.

The solar wind is the best example for studying unbounded collisionless plasmas in astrophysics. It is quite challenging to understand the behavior of such plasmas in the regime of turbulence, but surprisingly some simplicity seems to emerge from complexity with a fluid-like behavior (see, e.g., Meyrand et al. 2019; Wu et al. 2019). Space missions like the Parker Solar Probe and Solar Orbiter could also help in testing theoretical ideas.

ORCID iDs

Sébastien Galtier  <https://orcid.org/0000-0001-8685-9497>

References

- Alexandrova, O., Lacombe, C., Mangeney, A., Grappin, R., & Maksimovic, M. 2012, *ApJ*, 760, L21
 Banerjee, S., Hadid, L. Z., Sahraoui, F., & Galtier, S. 2016, *ApJL*, 829, L27

- Behannon, K. W. 1978, *RvGSP*, **16**, 125
- Biskamp, D., Schwarz, E., & Drake, J. 1996, *PhRvL*, **76**, 1264
- Boffetta, G., Celani, A., Dezzani, D., Laurie, J., & Nazarenko, S. 2009, *JLTP*, **156**, 193
- Boldyrev, S., & Perez, J. C. 2012, *ApJL*, **758**, L44
- Bourouaine, S., Alexandrova, O., Marsch, E., & Maksimovic, M. 2012, *ApJ*, **749**, 102
- Cerri, S. S., Califano, F., Jenko, F., Told, D., & Rincon, F. 2016, *ApJL*, **822**, L12
- Chen, C. H. K., Boldyrev, S., Xia, Q., & Perez, J. C. 2013, *PhRvL*, **110**, 225002
- Chen, C. H. K., Leung, L., Boldyrev, S., Maruca, B. A., & Bale, S. D. 2014, *GeoRL*, **41**, 8081
- Connaughton, C., & Nazarenko, S. 2004, *PhRvL*, **92**, 044501
- Denskat, K. U., Beinroth, H. J., & Neubauer, F. M. 1983, *JGZG*, **54**, 60
- Dyachenko, S., Newell, A. C., Pushkarev, A., & Zakharov, V. E. 1992, *PhyD*, **57**, 96
- Falkovich, G. E., & Shafarenko, A. V. 1991, *JNS*, **1**, 457
- Galtier, S. 2006a, *JPIPh*, **72**, 721
- Galtier, S. 2006b, *JLTP*, **145**, 59
- Galtier, S., & Bhattacharjee, A. 2003, *PhPI*, **10**, 3065
- Galtier, S., & Buchlin, É. 2010, *ApJ*, **722**, 1977
- Galtier, S., & Meyrand, R. 2015, *JPIPh*, **81**, 325810106
- Galtier, S., Nazarenko, S. V., Buchlin, E., & Thalabard, S. 2019, *PhyD*, **390**, 84
- Galtier, S., Nazarenko, S. V., Newell, A. C., & Pouquet, A. 2000, *JPIPh*, **63**, 447
- Hadid, L. Z., Sahraoui, F., & Galtier, S. 2017, *ApJ*, **838**, 9
- Kiyani, K., Osman, K., & Chapman, S. 2015, *RSPTA*, **373**, 20140155
- Kiyani, K. H., Chapman, S. C., Khotyaintsev, Y. V., Dunlop, M. W., & Sahraoui, F. 2009, *PhRvL*, **103**, 075006
- Leamon, R. J., Smith, C. W., Ness, N. F., Matthaeus, W. H., & Wong, H. K. 1998, *JGR*, **103**, 4775
- Leith, C. E. 1967, *PhFl*, **10**, 1409
- MacBride, B. T., Smith, C. W., & Forman, M. A. 2008, *ApJ*, **679**, 1644
- Matthaeus, W. H., Oughton, S., & Zhou, Y. 2009, *PhRvE*, **79**, 035401
- Meyrand, R., & Galtier, S. 2010, *ApJ*, **721**, 1421
- Meyrand, R., & Galtier, S. 2013, *PhRvL*, **111**, 264501
- Meyrand, R., Kanekar, A., Dorland, W., & Schekochihin, A. A. 2019, *PNAS*, **116**, 1185
- Narita, Y., Gary, S. P., Saito, S., Glassmeier, K.-H., & Motschmann, U. 2011, *GeoRL*, **38**, L05101
- Nazarenko, S. V. 2011, *Wave Turbulence*, Vol. 825 (Berlin: Springer)
- Osman, K. T., Wan, M., Matthaeus, W. H., Weygand, J. M., & Dasso, S. 2011, *PhRvL*, **107**, 165001
- Passot, T., & Sulem, P. L. 2015, *ApJL*, **812**, L37
- Passot, T., & Sulem, P. L. 2019, *JPIPh*, **85**, 905850301
- Passot, T., Sulem, P. L., & Tassi, E. 2018, *PhPI*, **25**, 042107
- Podesta, J. J. 2013, *SoPh*, **286**, 529
- Richardson, J. D., Paularena, K. I., Lazarus, A. J., & Belcher, J. W. 1995, *GeoRL*, **22**, 325
- Roberts, O. W., & Li, X. 2015, *ApJ*, **802**, 1
- Sahraoui, F., Goldstein, M. L., Belmont, G., Canu, P., & Rezeau, L. 2010, *PhRvL*, **105**, 131101
- Sahraoui, F., Huang, S. Y., Belmont, G., et al. 2013, *ApJ*, **777**, 15
- Salem, C. S., Howes, G. G., Sundkvist, D., et al. 2012, *ApJL*, **745**, L9
- Schekochihin, A. A., Cowley, S. C., Dorland, W., et al. 2009, *ApJS*, **182**, 310
- Sorriso-Valvo, L., Marino, R., Carbone, V., et al. 2007, *PhRvL*, **99**, 115001
- Thalabard, S., Nazarenko, S., Galtier, S., & Medvedev, S. 2015, *JPhA*, **48**, 285501
- Vasquez, B. J., Smith, C. W., Hamilton, K., MacBride, B. T., & Leamon, R. J. 2007, *JGRA*, **112**, 7101
- Voitenko, Y., & de Keyser, J. 2011, *NPGeo*, **18**, 587
- Wu, H., Verscharen, D., Wicks, R. T., et al. 2019, *ApJ*, **870**, 106
- Zakharov, V. E., & Pushkarev, A. N. 1999, *NPGeo*, **6**, 1